Supplementary Materials for

Local amplifiers of IL-4Rα–mediated macrophage activation promote repair in lung and liver

Carlos M. Minutti, Lucy H. Jackson-Jones,* Belén García-Fojeda,* Johanna A. Knipper, Tara E. Sutherland, Nicola Logan, Emma Rinqvist, Raquel Guillamat-Prats, David A. Ferenbach, Antonio Artigas, Cordula Stamme, Zissis C. Chroneos, Dietmar M. Zaiss, Cristina Casals,† Judith E. Allen†

*These authors contributed equally to this work.
†Corresponding authors. Email: judi.allen@manchester.ac.uk (J.E.A.); ccasalsc@ucm.es (C.C.)

Published 11 May 2017 on *Science* First Release
DOI: 10.1126/science.aaj2067

This PDF file includes:

Materials & Methods

Proteins

Surfactant protein A was isolated from bronchoalveolar lavage (BAL) of patients with alveolar proteinosis using a sequential butanol and octylglucoside extraction (*11, 30-33*). The purity of SP-A was checked by one-dimensional SDS-PAGE in 12 % acrylamide under reducing conditions and mass spectrometry. The oligomerization state of SP-A was assessed by electrophoresis under non-denaturing conditions (*31-33*), electron microscopy (*33*), and analytical ultracentrifugation as reported elsewhere (*32*). SP-A consisted of supratrimeric oligomers of at least 18 subunits. Each subunit had a relative molecular mass (Mr) of 36 kDa. Recombinant human SP-A1 ($SP\text{-}A1^{hyp}$) was expressed in insect cells and purified from the medium by mannose affinity chromatography (*31, 32*). The stability of $SP\text{-}A1^{hyp}$ collagen domain was assessed by circular dichroism (*31, 32*) and differential scanning calorimetry (*32*). The oligomerization state of $SP\text{-}A1^{hyp}$ was evaluated by electrophoresis under non-denaturing conditions (*31, 32*) and analytical ultracentrifugation (*32*). $SP\text{-}A1^{hyp}$ consists of trimers and hexamers. The endotoxin content of native or recombinant human SP-A was < 0.1 endotoxin units /mg of SP-A as determined by *Limulus* amebocyte lysate assay (GenScript, Piscataway, NJ). Levels of mouse SP-A from BAL, pleural exudate, or lung tissue were detected by Western blot analysis as reported elsewhere (*11, 30-33*). Native human C1q was obtained from Abcam (Cambridge, UK). C1q consists of octadecamers with a Mw 410 kDa.

Experimental animals

C57BL/6 WT and gene-targeted mice were used in this study. SP-A ($Sftpa1^{-/-}$) (*34*), C1q ($C1qa^{-/-}$) (*35*), IL-4Rα ($Il4ra^{-/-}$) (*36*) and myeloid-specific HIF-1α ($Hif1a^{flox/flox};LysMcre^{+/-}$) (*37*) deficient mice and WT mice were bred and maintained at the University of Edinburgh under specific-pathogen free conditions. Sex-matched mice were 6-8-weeks old at the start of the experiment, and all mice were housed in individually ventilated cages. $Sftpa1^{-/-}$ and $Sftpa1^{+/+}$ littermates were genotyped using specific primers (**Supplementary Table 1**). Mice were not randomized in cages, but each cage was randomly assigned to a treatment group. Investigators were not blinded to mouse identity during necropsy; however, the analysis of adult worms, eggs in feces, lung and peritoneal pathology were performed in a blinded fashion.

Experiments were performed in accordance with the United Kingdom Animals (Scientific Procedures) Act of 1986 and the Spanish guidelines for experimental animals. All researchers were accredited for animal handling and experimentation by the UK and Spanish government Home Office. Dispensation to carry out animal research at the University of Edinburgh was approved by the University of Edinburgh Animal Welfare and Ethical Review Body and granted by the UK government Home Office; as such all research was carried under the project licenses PPL60/4104, PPL70/8548 and PPL70/8470. Sample size was calculated on the basis of the number of animals needed for detection of macrophage proliferation in WT mice, based on published experiments (*38-40*). Data was not excluded under any circumstances.

Sprague Dawley rats (~350 g) were purchased from Harlan (Indianapolis, IN). All animal experiments were fully compliant with the regulations set by the local ethical committee. Animals were treated according to the Directive 2010/63/EU of The European Parliament and the Spanish Act RD53/2013 of 8th February 2013 on protection of animals used for experimentation and other scientific purposes.

***Nippostrongylus brasiliensis* infection**

Mouse-adapted *N. brasiliensis* was maintained by serial passage through C57BL/6 mice, as described previously (*41*). Mice were infected subcutaneously with 250 or 400 *N. brasiliensis* third-stage larvae. Analysis of samples was performed at day 6 post-infection. Egg output was analyzed in feces and adult worm burden was determined by removing the small intestine and exposing the lumen by dissection. For macrophage proliferation analysis, mice were injected with 100 µl of 10 mg/ml BrdU in Dulbecco's phosphate buffered saline 3h before experimental end point. The lungs and pleural cavities were washed to obtain the BAL and pleural exudate. Subsequently, the right lung was perfused and fixed for histology. Alternatively, one section of the left lung was stored for mRNA quantification; another section was homogenized to obtain single cell suspensions for flow cytometry analysis, and a third section was stored for SP-A quantification. In this case, lung tissue was homogenized in HBSS containing protease inhibitor cocktail (Sigma-Aldrich, St. Louis, MO). SP-A was detected in both lung homogenates and BAL by Western blot analysis using an anti-mouse SP-A (GeneTex, Inc, Irvine, CA). SP-A levels were normalized by BAL volume or GAPDH. Only samples on which the same BAL volume was recovered

were used for SP-A quantification.

BAL cells were obtained by washing the lung with Dulbecco's phosphate buffered saline containing 0.5% BSA (m/v). Cells from pleural or peritoneal exudate were obtained by washing either pleural or peritoneal cavity with RPMI 1640 containing 2 mM L-glutamine, 200 U/ml penicillin, 100 µg/ml streptomycin. Single cell suspensions of thoracic lymph node tissue were re-stimulated *ex vivo* with *N. brasiliensis* excretory secretory antigen (*42*) (1 µg/ml) or anti-CD3 (1 µg/ml), and cell supernatants were analyzed by ELISA 72 h later.

Listeria monocytogenes infection

Listeria monocytogenes infections were performed as previously described (*26*). Briefly, frozen stocks of *L. monocytogenes* (Lm10403s) were thawed and then diluted in fresh Brain-Heart-Infusion (BHI) medium to reach mid-log growth phase. Mice were intravenously injected via the lateral tail vein with 1 x10^4 *L. monocytogenes* c.f.u. suspended in 200 µl of phosphate-buffered saline (PBS). Analysis of samples was performed at day 3.5 post-infection. The livers were perfused in situ with PBS before collection. For macrophage activation and proliferation analysis, mice were injected with 100 µl of 10 mg/ml BrdU in Dulbecco's phosphate buffered saline 3h before experimental end point. One section of the liver was homogenized to obtain single cell suspensions for flow cytometry analysis, a second section of the liver was stored for mRNA quantification; a third section was stored for cytokine quantification by ELISA; and a fourth section was homogenized to analyze bacterial burden. To analyze cytokine secretion by ELISA, the liver tissue was weighed before homogenization in Hank's balanced salt solution (HBSS) containing protease inhibitor cocktail. To quantify bacterial burden, serial dilutions of cell suspensions in PBS were plated on BHI agar plates. After 24 hr of incubation at 37°C, colony-forming units were counted. To analyze liver damage, blood was collected from the inferior vena cava and alanine transaminase (ALT) and aspartate transaminase (AST) levels were determined in the serum.

Peritoneal fibrosis model

Peritoneal fibrosis was induced by continuous administration of Dianeal PD-4 (Baxter, Deerfield, IL), as described previously (*18*) with slight modifications. Mice received a total of 5 or 14 injections of 500 µl (~200 ml/kg) of Dianeal PD-4 (ip) on

alternate days. Animals were sacrificed a day after the last delivery. The right section of the parietal layer of the peritoneum was collected for histology analysis. The left section of the peritoneum was stored in RNAlater for subsequent analysis. Peritoneal macrophages were isolated from the peritoneal cavity as described below. Note: Although timing of macrophage activation and proliferation in this model varied slightly between males and females all animals developed peritoneal fibrosis after 14 injections.

Histology

The right lung lobes were perfused and fixed with 10% neutral buffered formalin, incubated overnight and transferred to 70% ethanol. Lungs were paraffin-embedded, sectioned and stained with hematoxylin and eosin (H&E). Linear means intercept (Lmi) method was used to quantify emphysema like damage (*43*). To calculate Lmi, 20 random non-overlapping fields (magnification x200) per H&E stained lung sample were taken. Six horizontal lines were drawn across each image (ImageJ 1.44) and the total number of alveolar wall intercepts counted per line. The length of each line was then divided by the number of intercepts to give the Lmi value. Images that included large bronchi and vessels were avoided and analysis was performed in a blinded and randomized fashion. With respect to histological analysis of the peritoneum tissue, the right parietal layer of the peritoneum was fixed with 10% neutral buffered formalin, incubated overnight and transferred to 70 % ethanol. Subsequently, peritonea were paraffin-embedded, sectioned and stained for Masson's trichrome. The thickness of the submesothelial compact zone was measured using ImageJ and this value was used to score the extent of peritoneal fibrosis. Five independent (×200) images were taken to examine the overall section. For each image, six horizontal lines were randomly drawn across the submesothelial compact zone to measure its thickness and the average value of each sample was used for analysis.

IL-4 complex delivery and in vivo blocking of Myo18A

IL-4 was delivered as a 2:1 molar ratio of recombinant mouse IL-4 (Peprotech, Rocky Hill, NJ) and anti-IL-4 mAb (clone 11B11; BioXcell, West Lebanon, NH) (*38, 39*). For pulmonary macrophage analysis, mice were injected ip with IL-4 complex (IL-4c) containing 5 μg of IL-4 and 25 μg of 11B11, or PBS vehicle control on days 0 and 2. Simultaneously, 50 μg of anti-Myo18A neutralizing antibody (provided by Dr Zissis

C. Chroneos (*16*)) or Rabbit IgG (R&D Systems, Minneapolis, MN) were delivered intra-nasally on days 2 and 3, and samples were collected on day 4. For studies of peritoneal macrophages, liver macrophages, and other tissue resident macrophage populations, mice received a single ip injection of 1 μg of IL-4 and 5 μg of 11B11, or PBS vehicle control. Anti-Myo18A neutralizing antibody (*16*) or Rabbit IgG (100 μg) was delivered 2 hr before IL-4c injection and samples were collected 24 hr later. Mice received a pulse of BrdU 3 hr before experimental end point. Bronchoalveolar, pleural and peritoneal cavity lavages as well as lung and liver tissue collection were performed as described above.

RNA extraction and quantitative real-time PCR

A section of the left lung, liver or parietal peritoneum was stored in RNAlater (Ambion, Carlsbad, CA). Tissue was homogenized in Trizol (Invitrogen, Carlsbad, CA) with a TissueLyser (Qiagen, Hilden, Germany). Similarly, human alveolar macrophages were collected with Trizol, and RNA was prepared according to manufacturer's instructions. Reverse transcription was performed using 1 μg of total RNA, 50 U Tetro reverse transcriptase (Bioline, London, UK), 40 mM dNTPs (Promega, Fitchburg, WI), 0.5 μg Oligo dT15 (Roche, Basel, Switzerland), and RNasin inhibitor (Promega). Transcript levels of genes of interest were measured by real-time PCR with the Lightcycler 480 II system (Roche) using SYBR Green I Master kit and specific primers **(Supplementary Table 2)** as previously described (*43*). Transcript levels of C1qa mRNA were measured using Taqman Master kit and the primers Mm00432142 (Applied Biosystems, Carlsbad, CA). PCR amplification was analyzed using 2nd derivative maximum algorithm (LightCycler 480 Sw 1.5, Roche) and the expression of the gene of interest was normalized to a housekeeping gene *Rn18s*, *Rpl13a*, or *GAPDH*. In the case of human alveolar macrophages, cells from at least 8 humans were used for all groups.

Flow Cytometry

Single cell suspensions from left lung, liver and other tissues were prepared by digesting with 80 U/ml DNase (Life Technologies, Carlsbad, CA) combined with 0.2 U/ml liberase TL (Roche) in HBSS at 37°C for 30 minutes. In some cases, liberase was combined with collagenase B (0.2 mg/ml) and D (0.4 mg/ml) (Roche). Tissue was homogenized by forcing through a 70 μM cell strainer. Cells from tissue

homogenates, BAL, pleural exudate, and peritoneal cavity exudate were treated with red blood cell lysis buffer (Sigma-Aldrich) and counted using an automated cellometer T4 (Peqlab, Radnor, PA). Cells were incubated with Fc block (CD16/CD32 and mouse serum) (BD Biosciences, Franklin Lakes, NJ) and stained with fluorescent conjugated antibodies to CD19 (clone 6D5; Biolegend, Cambridge, UK), Siglec F (clone E50-2440; BD Biosciences), Ly6G (clone 1A8; Biolegend), CD3 (clone 17A2; Biolegend), CD45.2 (clone 104; Biolegend), Ly6C (clone HK1.4; Biolegend), CD11c (clone N418; Biolegend), CD11b (clone M1/70; Biolegend), F4/80 (clone BM8, eBiosciences, Hatfield, UK), I-A/I-E (MHCII) (clone M5/114.15.; eBiosciences), CD102 (clone 3C4 (MIC2/4); Biolegend), GATA6 (ref. D61E4; Cell Signaling, Danvers, MA), TER119 (clone TER-119; Biolegend), CD4 (clone RM4-5; Biolegend), FcεR1 (clone MAR-1; Biolegend), NK-1.1 (clone PK136; Biolegend), CD90.2 (clone 30-H12; Biolegend), ICOS (clone C398.4A; Biolegend) and unconjugated anti-Myo18A antibody (*16*) (5 μg/ml) or isotype control followed by secondary reagents (Invitrogen). The following surface markers identified alveolar macrophages: lineage$^-$ (CD19, Ly6G, CD3 and TER119), Ly6C$^-$, CD45.2$^+$, CD11c$^+$ and SiglecF$^+$. Peritoneal, pleural, and liver macrophages as well as other tissue resident macrophages were identified as lineage$^-$ (CD19, SiglecF, Ly6G and CD3), CD11c$^-$, Ly6C$^-$, CD45.2$^+$, CD11b$^+$ and F4/80$^{+\text{ or high}}$ (*38*). ILC2 cells were identified as lineage$^-$ (CD3, CD11b, CD11c, FcεR1, CD19, and NK1.1) CD90.2$^+$ ICOS$^+$ CD45.2$^+$ cells. T helper cells were identified as CD45.2$^+$, CD3$^+$ and CD4$^+$. Neutrophils were identified as CD45.2$^+$, CD11b$^+$ and Ly6G$^+$. Monocytes were identified as CD45.2$^+$, CD11b$^+$ and Ly6C$^+$.

Following surface staining, cells were fixed with 2% paraformaldehyde in Dulbecco's phosphate buffered saline for 20 min at room temperature, permeabilized with Perm wash (BD Biosciences), and then stained with anti-RELMα, biotinylated anti-Ym1, APC-conjugated anti-Arg-1 (R&D Systems), or isotype control followed by secondary reagents (Invitrogen). For detection of Ki67 and measurement of BrdU incorporation, cells were stained for surface markers, then fixed and permeabilized using FoxP3 staining buffer set (eBioscience), and subsequently stained with Ki67 set (clone BV56, BD Biosciences) or anti-BrdU (clone BU20a, Biolegend) for 30 min at room temperature. Cells were incubated first with or without DNase for 30 min at 37ºC before staining with anti-BrdU antibody. For intracellular cytokine staining, lung single cell suspensions were re-stimulated ex vivo in complete RPMI1640 media

(supplemented with 10% FCS, 2 mM L-glutamine, 100 U/ml penicillin, 100 µg/ml streptomycin) containing 1 µg/ml ionomycin, 500 ng/ml PMA, and 10 µg/ml Brefeldin A for 4 hr at 37°C. Following surface staining and fixing, cells were intracellularly stained with anti-IL-4 (clone 11B11, Biolegend), IL-13 (clone eBio13A; eBiosciences), IL-5 (clone TRFK5; Biolegend), and relevant isotypes. Expression of RELMα, Ym1, Arg-1, Ki67, IL-4, IL-13, and IL-5 was determined relative to isotype control staining. Incorporation of BrdU was determined relative to staining of non-DNase treated cells. Live/Dead (Life Technologies) was used to exclude dead cells from analysis. Samples were analyzed by flow cytometry using Becton-Dickinson FACS LSR II and FlowJo software.

ELISAs

Quantification of RELMα (PeproTech) and Ym1 (R&D Systems) were performed by ELISA in BAL, pleural and peritoneal exudates, as well as in cell supernatants of *ex vivo* cultures of peritoneal or alveolar macrophages. IL-4, IL-5, IL-13, TNF-α, and IFN-γ (BioLegend and eBioscience) were measured in supernatants of *ex vivo* re-stimulated thoracic lymph node cells and liver homogenates. C1q quantification was performed by ELISA (Source BioScience, Nottingham, UK) in peritoneal cavity exudates. ELISA assays were performed following manufacturer's instructions.

Isolation and culture of primary alveolar, peritoneal, and liver macrophages

Alveolar macrophages were obtained from BAL of mice and rats, and from human lung biopsies obtained from patients that were submitted to a pulmonary lobectomy. An informed consent was obtained from all donors. The review board and the ethics committee of the Sabadell Hospital approved this study, which was conducted in accordance with the guidelines of the World Medical Association's Declaration of Helsinki. BAL was performed with Dulbecco's phosphate buffered saline with or without 0.2 mM EDTA and 0.5% BSA (m/v). Macrophages were purified by adherence for at least 90 min at 37°C, and 5% CO_2 as previously reported (*44*). Adherent cells were 94.0 ± 1.1 % viable (trypan blue exclusion test). Flow cytometry analysis determined that 90 ± 1 % of adherent cells isolated from BAL were CD11c and SiglecF positive. To estimate the purity of isolated human macrophages, cells were cytospun in a CytoSpin 3 Cytocentrifuge (Shandon Scientific, Waltham, MA), and the cytospin preparations were stained either with anti-CD68 or Diff-Quick kit

(Diagnostics Grifols, Barcelona, Spain) following the manufacturer's protocol. 95 % ± 1.5 % (n=6) of adherent cells were macrophages.

Peritoneal macrophages were obtained from mice by washing the peritoneal cavity with RPMI 1640 containing 2 mM L-glutamine, 200U/ml penicillin, 100 µg/ml streptomycin. For thioglycollate-induced macrophages, mice were injected with 0.4 ml of 4% Brewer's thioglycollate (Sigma-Aldrich) for 48–96 h before peritoneal cells were harvested. Cells were separated from the lavage fluid by centrifugation (250 x g, 5 min), resuspended in RPMI 1640 medium (5% heat-inactivated FBS, 100 U/ml penicillin, 100 µg/ml streptomycin, supplemented with 2 mM glutamine), and purified by adherence. Viability of adherent cells was assessed by trypan blue exclusion test. Flow cytometry analysis determined that 90 ± 1 % of adherent cell isolated from the peritoneal exudate were F4/80 and CD11b positive.

Liver macrophages were isolated from mouse livers as reported previously (*45*) with some modifications. Before collection of the tissue, mice were culled and bled by cutting the inferior vena cava. Subsequently the liver was perfused in situ with PBS. The liver was then excised and kept in HBSS. Subsequently, the organ was minced to small pieces and digested with collagenase B (0.2 mg/ml), collagenase D (0.4 mg/ml) (Roche) and 80 U/ml DNase (Life Technologies) in HBSS at 37°C for 30 minutes. Digested tissue was filtered through a cell strainer (70 µm) to prepare a single cell suspension. The filtrate was centrifuged twice at 300xg (4°C) for 5 min to wash out the residual enzymatic solution. The pellet was resuspended and centrifuged at 50xg (4°C) for 3 min to separate non-parenchymal from parenchymal cells. The pellet containing parenchymal cells was discarded. The supernatant was centrifuged again at 300xg for 5 min. The cell pellet was seeded on 96-well culture plates in complete culture medium [RPMI 1640 medium (10% heat-inactivated FBS, 100 U/ml penicillin, 100 µg/ml streptomycin, supplemented with 2 mM glutamine)]. Following incubation for 2 h in a humidified atmosphere of 95% air with 5% carbon dioxide (CO_2) at 37°C, the cells were gently washed with fresh culture medium. Viability of adherent cells was assessed by trypan blue exclusion test. Flow cytometry analysis determined that 70 ± 5 % of adherent cells isolated from the liver homogenates were F4/80 and CD11b positive.

In vitro stimulation of macrophages

Macrophages were pre-cultured for 24 h in RPMI 1640 medium with 5% FBS. Subsequently, cells were treated with IL-4 (0.5-1 µg/ml) (ImmunoTools, Friesoythe, Germany) and/or SP-A (25, 50 and 100 µg/ml) or native human C1q (10 and 100 µg/ml). The following blocking antibodies were added 2 h before stimulation: 10 µg/ml of anti-Myo18A (*16*), 10-50 µg/ml anti-SIRPα (eBioscience), and 10-50 µg/ml anti-calreticulin (Thermo Scientific, Waltham, MA). Under these conditions, cell viability was higher than 97%. Macrophage cultures were plated in triplicate wells and each series of experiments was repeated at least three times.

Cell proliferation assays

For 5–ethynyl–2′–deoxyuridine (EdU)/BrdU incorporation analysis, cells were treated with IL-4, SP-A, C1q and combinations thereof for 24 h. Then, cells were exposed to 10 µM EdU/BrdU for another 24 h. For confocal microscopy analysis of EdU incorporation, cells were fixed with 2% formaldehyde for 15 minutes at room temperature and permeabilized with 0.2% saponin in PBS. EdU was detected with Alexa Fluor 647-azide using Click-iT EdU assay kit (Life Technologies). Sequential double immunostaining was performed with a monoclonal antibody to CD11c (AbD Serotec, Kidlington, UK), and immune complexes were visualized with FITC-conjugated secondary antibody (Invitrogen). Micrographs were taken with a Leica TCS SP2 Confocal System. Flow cytometry analysis of BrdU and Ki67 expression was performed as described above.

Arginase activity assay

Arginase activity was measured as previously reported (*46*). Briefly, rat alveolar macrophages were lysed with 50 µl of 50 mM Tris–HCl pH 7.5, 0.1 % Triton X-100, 1 mM benzamidine, 200 µg/ml aprotinin, and 200 µg/ml leupeptin. After 30 min shaking at 4ºC, arginase was activated with 50 µl of 10 mM $MnCl_2$ and 50 mM Tris-HCl, pH 7.5, for 10 min at 55º C. L-arginine hydrolysis was measured by incubating the cell lysate with 25 µl of 0.5 M L-arginine (Sigma-Aldrich) (pH 9.7) at 37ºC for 1 h. The reaction was stopped by addition of 200 µl H_2SO_4 /H_3PO_4 /H_2O (1:3:7 v/v). The produced urea was quantified at 570 nm after addition of 25 µl of α-isonitrosopropiophenone (dissolved in 100% ethanol) followed by heating at 99ºC for 45 min. Urea production was normalized to cell number for each treatment by

quantifying cells with the WST-1 reagent (Roche), following manufacturer's instructions. One unit of arginase activity is defined as the amount of enzyme that catalyses the formation of 1 µmol urea per min.

siRNA-mediated gene-silencing effects in vitro

After isolation, primary alveolar macrophages were resuspended in Amaxa® mouse macrophage nucleofector solution (Lonza, Basel, Switzerland) and nucleofected with 100 nM siRNA using a nucleofector 2b device (Lonza). Experiments were conducted using two Stealth siRNAs directed against rat Myo18A (RSS322720 and RSS322721) (Applied Biosystems). Medium GC Stealth siRNA was used as control (12935300) (Applied Biosystems). Myo18A expression was detected by Western blot analysis with an anti-Myo18A antibody (*16*). After 48 hr post nucleofection, Myo18A expression was reduced 72 ± 4% for RSS322720 and 71 ± 5% for RSS322721 compared to control. At this time point, cells were stimulated.

Statistics

Normal distribution of data was determined by visual examination of residuals. Statistical evaluation of different groups was performed either by analysis of variance (ANOVA) followed by the Bonferroni multiple comparison test or by unpaired two-tailed Student's t-test, as indicated. An α level ≤ 5% ($p \leq 0.05$) was considered significant. All statistical calculations were performed using PRISM, (Graphpad, La Jolla, CA).

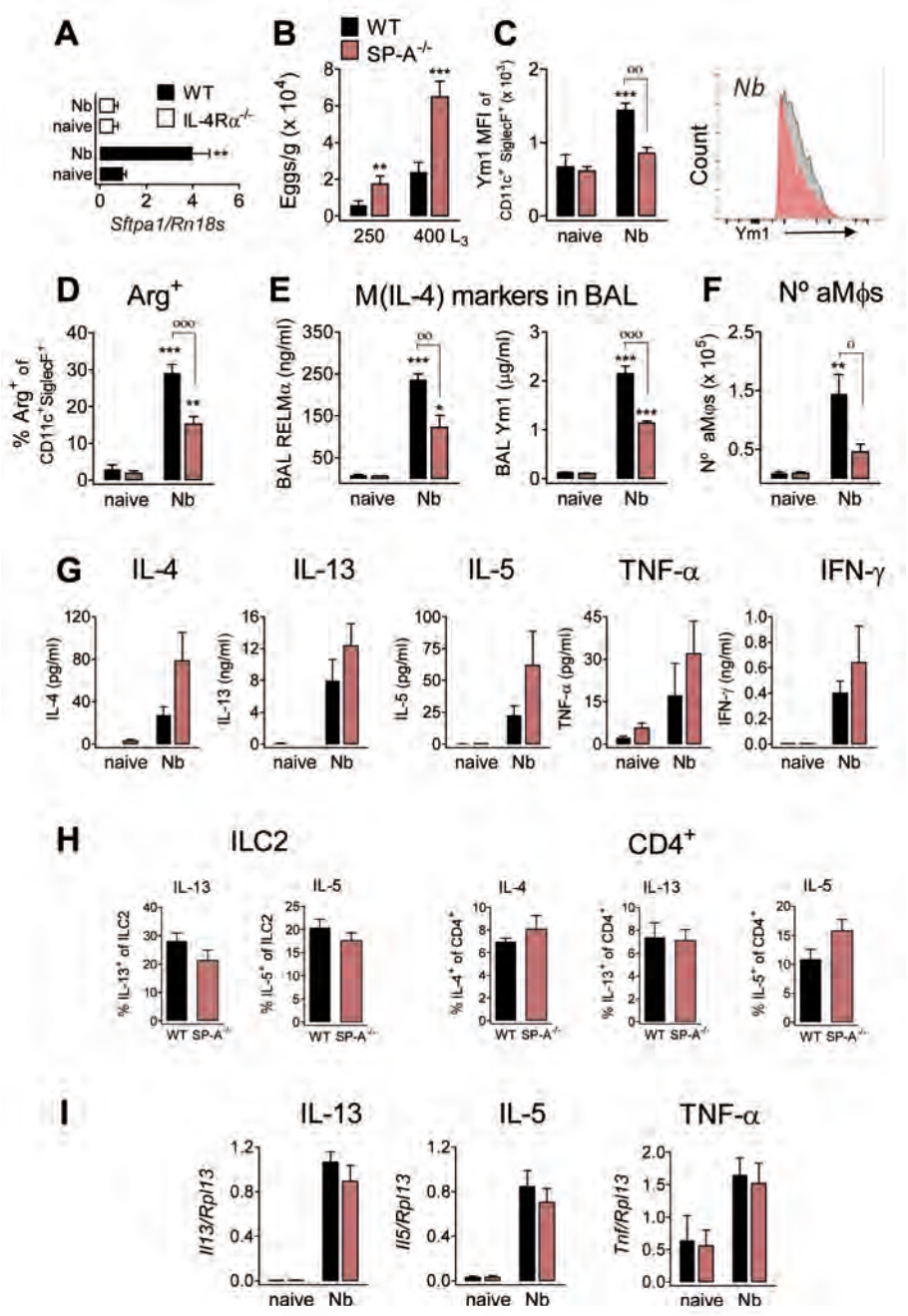

Fig. S1. Further characterization of WT vs. SP-A-deficient mice during *Nippostrongylus brasiliensis* infection. WT or SP-A$^{-/-}$ mice were left uninfected or infected with 250 *N. brasiliensis* L3's, and assessed at day 6 after infection. **(A)** SP-A mRNA expression in lung tissue of WT and IL-4Rα$^{-/-}$ mice. **(B)** Egg output in feces form WT and SP-A$^{-/-}$ mice. Expression of **(C)** Ym1 and **(D)** Arg by aMϕ . **(E)** Analysis of secreted RELMα and Ym1 from BAL by ELISA. **(F)** Number of alveolar macrophages recovered in BAL. **(G)** Levels of IL-4, IL-13, IL-5, TNFα, and IFN-γ in supernatants of thoracic lymph node cells from WT and SP-A$^{-/-}$ mice, cultured with *N. brasiliensis* antigen (1 μg/ml); results are normalized to those obtained for cells cultured with medium alone. **(H)** Expression of IL-13 and IL-5 by ILC2 and IL-4, IL-13 and IL-5 by CD4^{+} cells from single-cell suspensions of lung tissue stimulated *ex vivo* with PMA and ionomycin. **(I)** Amplification of *Il13*, *Il5* and *Tnf*-encoding mRNA in lung homogenates is also shown. Results are representative from two independent experiments (means ± SEM) (naïve: 3 mice, *Nb*: 6 mice). ANOVA followed by the Bonferroni multiple-comparison test or Student's *t*-test (F) was used. **P* < 0.05 , ***P* < 0.01 and ****P* < 0.001, when compared with the uninfected group; °*P* < 0.05, °°*P* < 0.01 and °°°*P* < 0.001 when WT vs. SP-A$^{-/-}$ infected groups are compared.

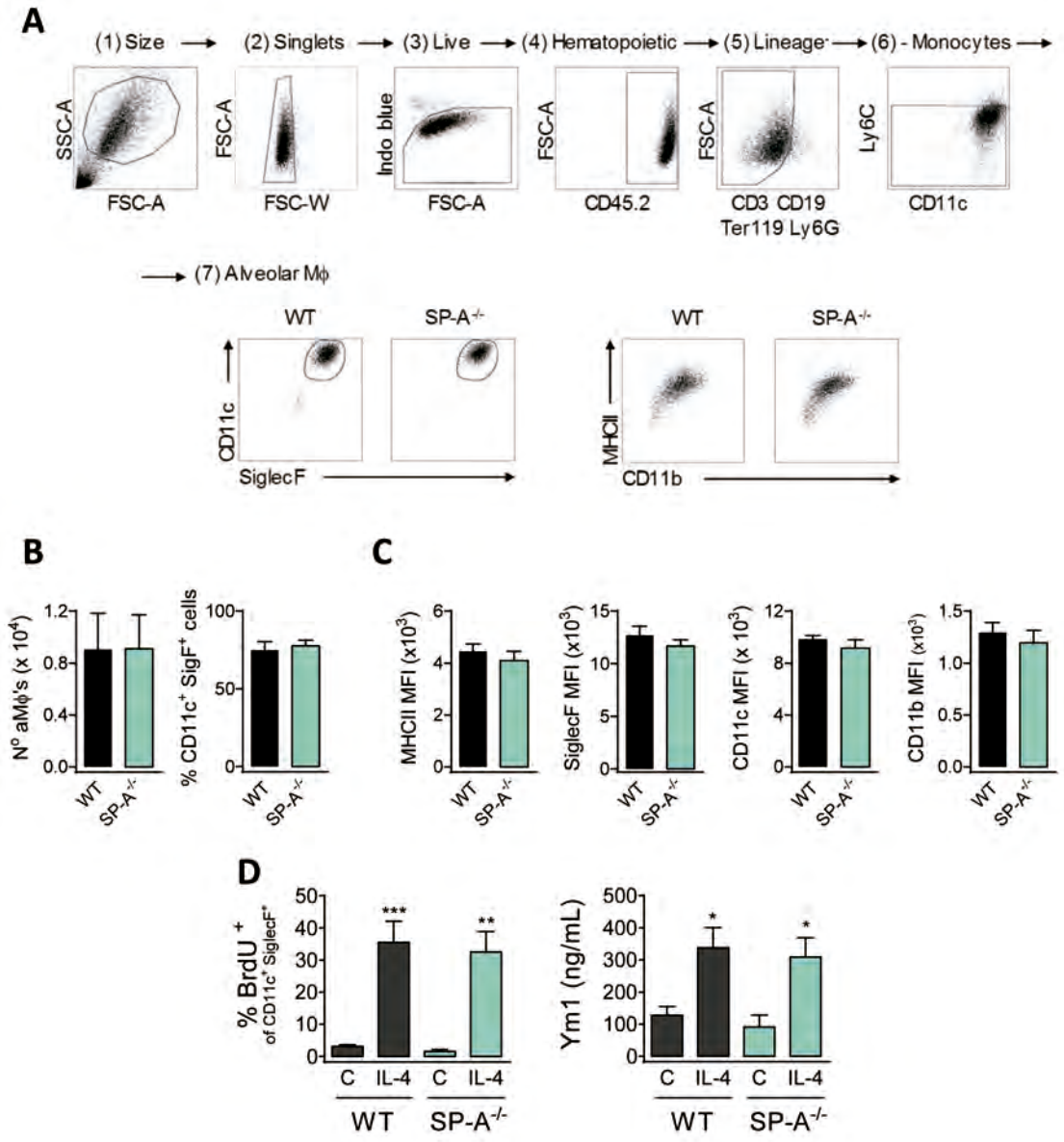

Fig. S2. Characterization of alveolar macrophages from SP-A-deficient mice. (A) Sequential identification of aMϕs by flow cytometry. Cells first identified by size (1), and then as singlets (2) and live cells (3). Subsequently, hematopoietic cells were selected by CD45.2 expression (4). Lin− cells (5) were obtained by gating out CD3+, CD19+, Ly6G+, and Ter119+ cells (T cells, B cells, neutrophils and red blood cells, respectively). Monocytes were successively excluded by expression of Ly6C (6). Lin− and Ly6C− populations were further subgated on the basis of the expression of CD11c versus SiglecF. aMϕ are identified as $CD11c^{hi}$ and $SiglecF^{hi}$ (7); a representative population of aMϕ from WT and SP-A-deficient mice is shown. The expression of MHCII and CD11b by aMϕs is also shown for both strains. All shown gates are children of the parent gates shown previously. **(B)** Number and percentage of aMϕ recovered in BAL. **(C)** Expression of MHCII, SiglecF, CD11c and CD11b in aMϕ from WT and SP-A-deficient mice. Data are representative from two independent experiments (mean ± SEM; WT: 4 mice, $SP\text{-}A^{-/-}$: 3 mice). Student's *t*-test was used. **(D)** Purified aMϕ from WT and SP-A-deficient mice were treated with or without IL-4 (1μg/ml) and exposed to BrdU for proliferation analysis. BrdU incorporation and secretion of Ym1 by resident aMϕ are shown. The results are presented as means (± SEM) from two different cell cultures with at least three biological replicates. ANOVA followed by the Bonferroni multiple-comparison test was used. $*P < 0.05$, $**P < 0.01$, and $***P < 0.001$, when compared with untreated macrophages.

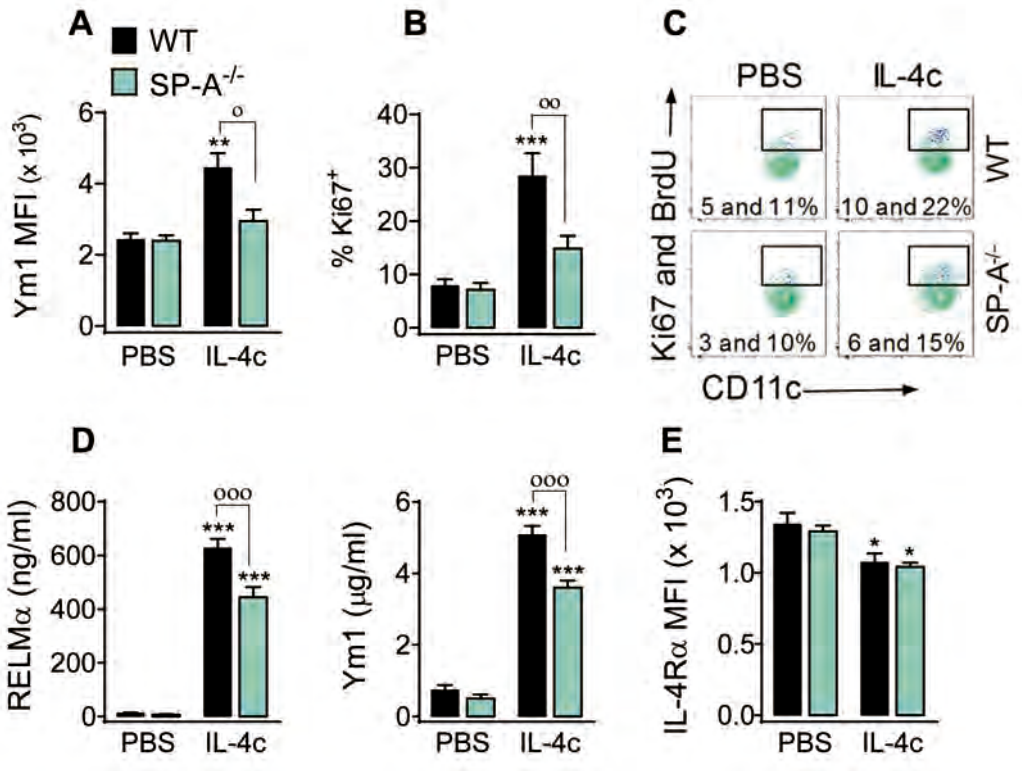

Fig. S3. Alveolar macrophages from SP-A-deficient mice show decreased IL-4-induced proliferation and M(IL-4) activation. WT and SP-A$^{-/-}$ mice were treated with 5μg of IL-4c (i.p.) at days 0 and 2; and samples were analyzed at day 4. **(A)** Ym1 and **(B)** Ki67 expression in aMϕ in response to IL-4c. In **(C)** a representative FACS plot from WT and SP-A$^{-/-}$ mice is shown to demonstrate overlap between BrdU^{+} and Ki67^{+} cells treated with PBS or IL-4c (Ki67 green contour and BrdU+ cells blue dots). **(D)** Protein levels of RELMα and Ym1 in BAL measured by ELISA. **(E)** Expression of IL-4Rα by aMϕ from BAL. Data were pooled from three independent experiments (means ± SEM) (PBS: 9 mice, IL-4c: 11 mice). ANOVA followed by the Bonferroni multiple-comparison test was used. **P* < 0.05, ***P* < 0.01, and ****P* < 0.001 when compared with the untreated group. °*P* < 0.05, °°*P* < 0.01 and °°°*P* < 0.001 when WT vs. SP-A$^{-/-}$ groups are compared.

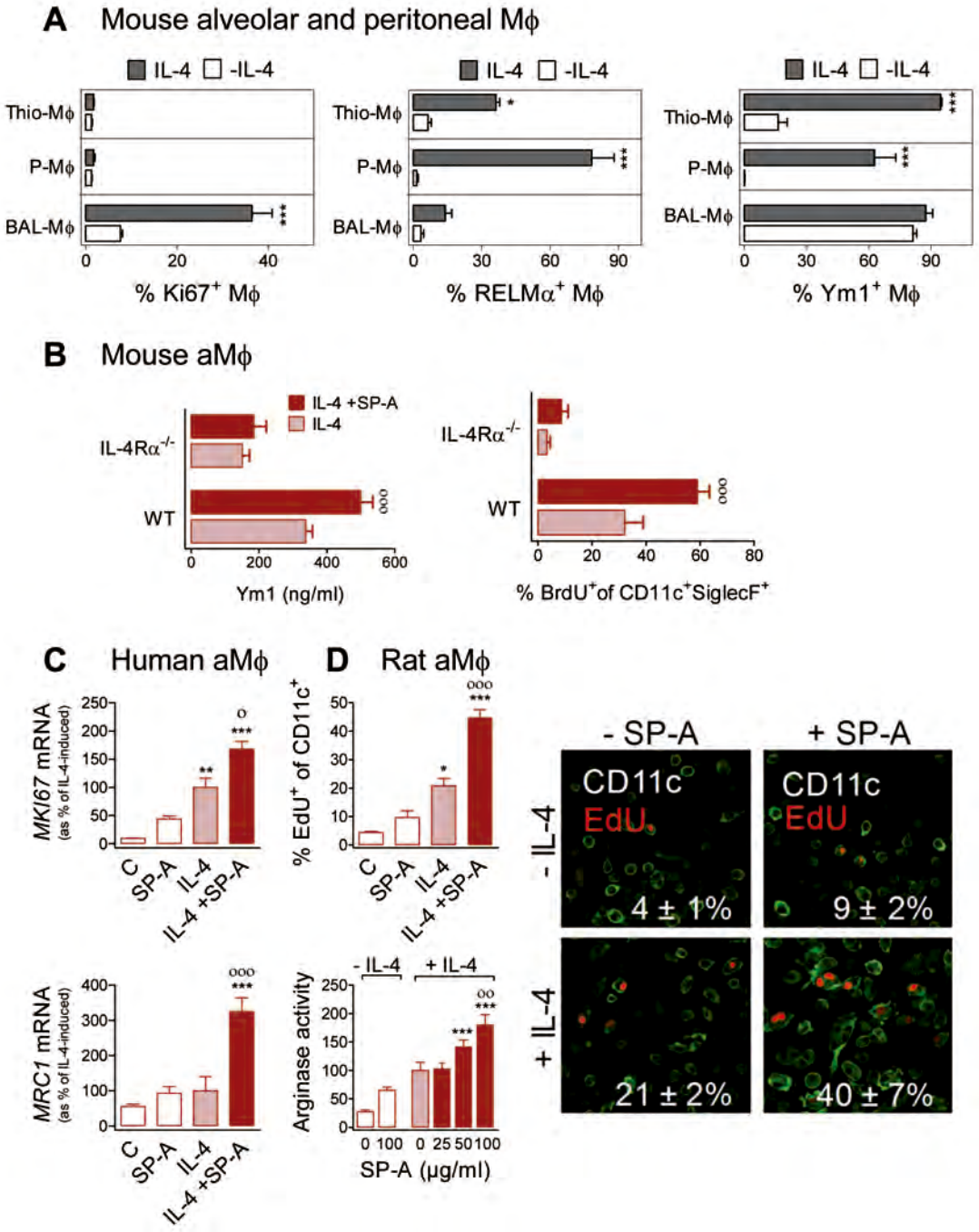

Fig. S4. Proliferation and activation of macrophages isolated from mice, humans, and rats. (A) Purified alveolar (BAL-Mϕ), peritoneal [resident (P-Mϕ)] and thioglycollate-recruited (Thio-Mϕ) from mice were treated with or without IL-4 (0.5-1 µg/ml). Ki67, RELMα, and Ym1 expression was assessed by FACS. Note: cultured aMϕ are $Ym1^+$ regardless of IL-4 treatment. Purified aMϕ from mice **(B)**, humans **(C)**, or rats **(D)** were treated with or without IL-4 (0.5-1 µg/ml) in the presence or absence of SP-A. (**B**) BrdU incorporation and secretion of Ym1 by cultured aMϕ from WT and IL-4Rα$^{-/-}$ mice in the presence and absence of SP-A. **(C)** *MKI67* and *MRC1* mRNA expression by human aMϕ as measured by qRT-PCR. (**D**) EdU incorporation analyzed by flow cytometry and arginase activity of rat aMϕ. A representative confocal micrograph of rat aMϕ immuno-stained with CD11c-FITC and EdU-Alexa Fluor 647 is shown. Numbers below indicate percentage ± SEM of EdU^+ cells from three independent experiments. The results are presented as means (± SEM) from three different cell cultures with at least three biological replicates. ANOVA followed by the Bonferroni multiple-comparison test was used. **P* < 0.05, ***P* < 0.01, and ****P* < 0.001, when compared with untreated macrophages; °*P* < 0.05, °°*P* < 0.01, and °°°*P* < 0.001, when SP-A+IL-4-treated macrophages were compared with IL-4-treated macrophages.

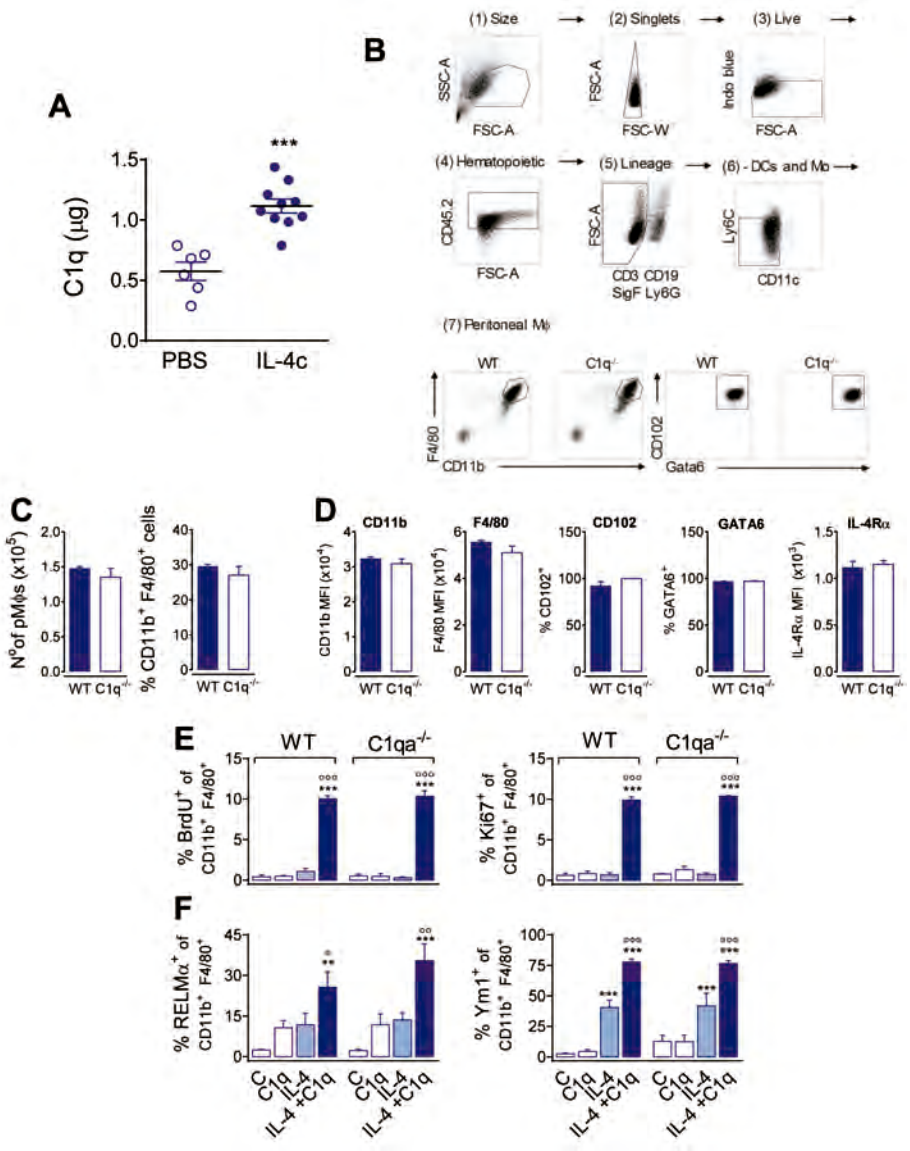

Fig. S5. C1q protein levels in the peritoneal cavity and characterization pMϕ of from C1q-deficient mice. (A) Following IL-4c delivery, C1q protein was measured by ELISA in WT mice. **(B)** Sequential identification of pMϕ by flow cytometry. Cells first identified by size (1), and then as singlets (2) and live cells (3). Subsequently, hematopoietic cells were selected by CD45.2 expression (4). Lin^- cells (5) were obtained by gating out $CD3^+$, $CD19^+$, $Ly6G^+$ and $SiglecF^+$ cells (T cells, B cells, neutrophils and eosinophils, respectively). Monocytes and dendritic cells were successively excluded by expression of Ly6C and CD11c (6). Lin^-, $CD11c^-$ and $Ly6C^-$ populations were further subgated on the basis of the expression of CD11b versus F4/80. pMϕ are $CD11b^{hi}$ and $F4/80^{hi}$ (7); a representative population of pMϕs from WT and C1q-deficient mice is shown. The expression of CD102 and Gata6 by pMϕs is also shown for both strains. All shown gates are children of the parent gates shown previously. **(C)** Number and percentage of pMϕ recovered in the peritoneal washes. **(D)** Expression of CD11b, F4/80, CD102, Gata6, and IL-4Rα in pMϕ from WT and C1q-deficient mice. Data are representative from two independent experiments (mean ± SEM; WT: 4 mice, $C1qa^{-/-}$: 4 mice). In C and D, Student's *t*-test was used. In E and F, purified pMϕ from WT and C1q-deficient mice were treated with or without IL-4 (1 µg/ml or 10 ng/ml) in the presence or absence of C1q, and exposed to BrdU. **(E)** Proliferation (BrdU incorporation and Ki67 expression) in response to 1 µg/ml of IL-4. **(F)** M(IL-4) activation (RELMα and Ym1 expression) of pMϕs in response to 10 ng/ml of IL-4. The data shown are means ± SEM of two different pMϕ cultures with at least three biological replicates. ANOVA followed by the Bonferroni multiple-comparison test was used. $^{**}P < 0.01$, and $^{***}P < 0.001$, when compared with untreated cells (C); $^{\circ}P < 0.05$, $^{\circ\circ}P < 0.01$, and $^{\circ\circ\circ}P < 0.001$, when C1q+IL-4-treated macrophages were compared with IL-4-treated macrophages.

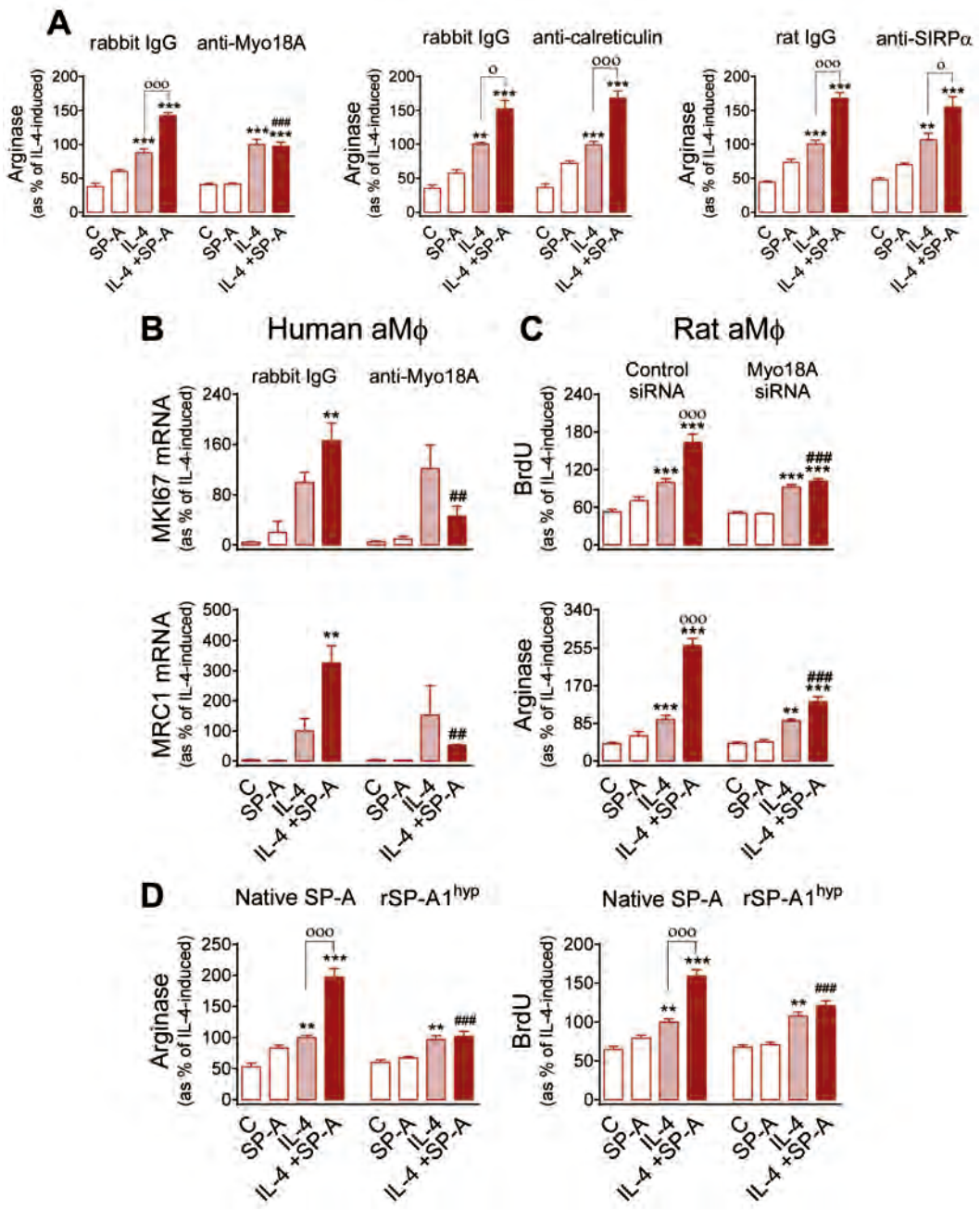

Fig. S6. (A-C) Myo18A mediates SP-A's effects on aMϕs isolated from humans and rats. (A) Purified rat aMϕ were treated with either anti-Myo18A (10 μg/ml), anti-calreticulin (10-50 μg/ml), anti-SIRPα (10-50 μg/ml), or an isotype control for two hours. Next, cells were IL-4-stimulated with or without native SP-A. **(B)** mRNA expression of *MKI67* and *MRC1* by human aMϕ treated with anti-Myo18A antibody. **(C)** BrdU incorporation and arginase activity in rat aMϕ that were nucleofected with Myo18A (RSS322720) or control siRNA. Similar results were found using RSS322721 Myo18A siRNA. **(D) The collagen-like domain of SP-A is required for functional interaction with Myo18A on aMϕ.** Purified rat aMϕ were IL-4-stimulated with or without either native human SP-A or recombinant human SP-A1 expressed in insect cells (SP-A1^{hyp}). Recombinant human SP-A1 expressed in insect cells lacks the prolyl hydroxylation, resulting in improper folding of the collagen domain (31). The data shown are means ± SEM of three different alveolar or pMϕ cultures with at least three biological replicates. ANOVA followed by the Bonferroni multiple-comparison test was used. $^{**}P < 0.01$, and $^{***}P < 0.001$, when compared with untreated cells (C); $^{\circ}P < 0.05$, and $^{\circ\circ\circ}P < 0.001$, when SP-A+IL-4-treated macrophages were compared with IL-4-treated macrophages; $\#\#P < 0.01$, and $\#\#\#P < 0.001$, when either the effect of Myo18A siRNA vs. control siRNA or anti-Myo18A vs. rabbit IgG are compared or when the effects of native SP-A vs. SP-A1^{hyp} on macrophage activation and proliferation are compared.

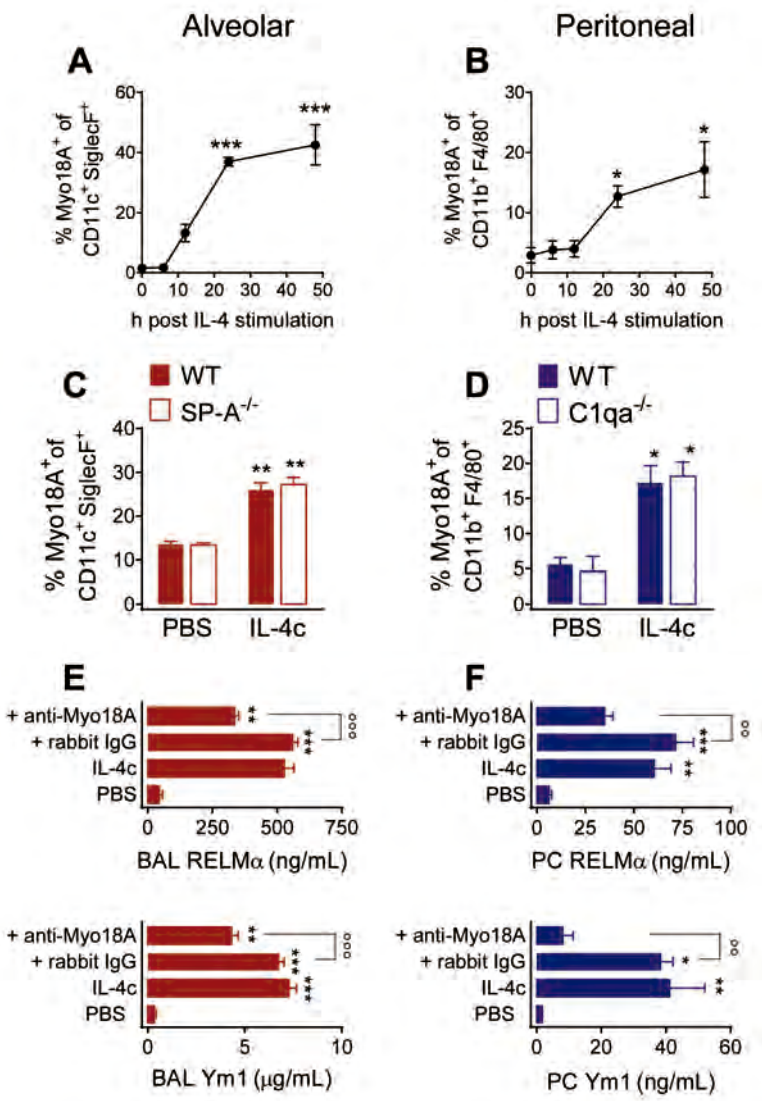

Fig. S7. Myo18A expression in response to IL-4 treatment and further characterization of blocking Myo18A on IL-4-mediated activation of macrophages *in vivo*. Time-dependent expression of Myo18A on the cell surface of alveolar **(A)** and peritoneal **(B)** macrophages in response to IL-4 treatment *in vitro*. The data shown are means ± SEM of three different aMϕ or pMϕ cultures with at least three biological replicates. ANOVA followed by the Bonferroni multiple-comparison test was used. **P* < 0.05, and ****P* < 0.001, when compared with 0 hours post IL-4 stimulation. **(C-D)** For aMϕs, 5 μg IL-4c was delivered ip at day 0 and day 2, and BAL cells analyzed at day 4. For pMϕs, 1 μg IL-4c was delivered ip at day 0, and peritoneal cells analyzed at day 1: Myo18A expression on the surface of macrophages from WT, SP-A$^{-/-}$, and C1qa$^{-/-}$ mice treated with or without IL-4c. **(E)** For aMϕs, mice were treated as in (C-D) and simultaneously, animals were intra-nasally treated with either anti-Myo18A or rabbit IgG at day 2 and 3, and lung samples were analyzed at day 4. **(F)** Alternatively, for pMϕs, mice were also treated as in (C-D) with concomitant delivery of anti-Myo18A or rabbit IgG (ip) 2 hours before IL-4c administration. Concentration of RELMα and Ym1 in BAL **(E)** and the peritoneal cavity (PC) **(F)** are shown. Data were pooled from three independent experiments (means ± SEM) (PBS: 6 mice, other groups: 9 mice). ANOVA followed by the Bonferroni multiple-comparison test was used. **P* < 0.05, ***P* < 0.01, and ****P* < 0.001, when compared with PBS treated mice; °°*P* < 0.01, and °°°*P* < 0.001 when anti-Myo18A vs rabbit IgG treatment is compared in IL-4c-treated mice.

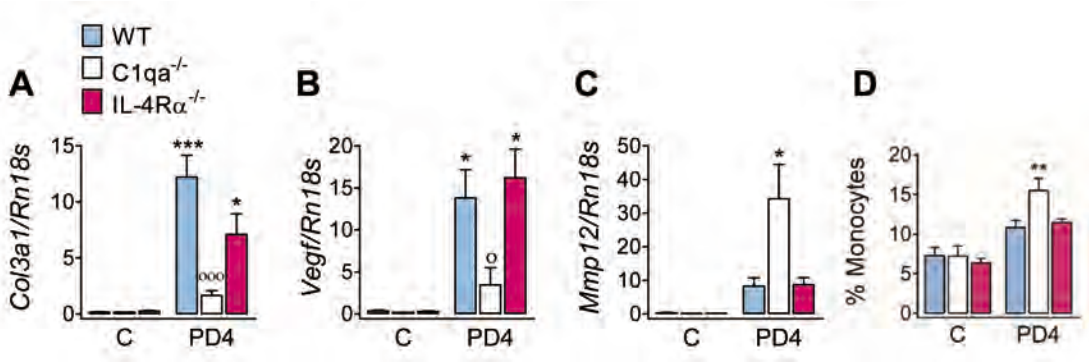

Fig. S8. Further characterization of WT , IL-4Rα and C1q-deficient mice in a model of peritoneal dyalisis. WT, C1qa$^{-/-}$ or IL-4Rα$^{-/-}$ mice were either untreated (control, C) or treated with 14 ip injections of Dianeal PD-4 every other day. Samples were analyzed a day after the last delivery. Amplification of **(A)** *Col3a1*, **(B)** *Vegf,* and **(C)** *Mmp12*- encoding mRNA in peritoneal tissue. **(D)** Percentage of infiltrating monocytes as quantified by FACS. Results are representative from two independent experiments (means ± SEM) (untreated: 3 mice, PD4: 6 mice). ANOVA followed by the Bonferroni multiple-comparison test or Student's t-test (A) was used. **P* < 0.05, ***P* < 0.01, and ****P* < 0.001 when compared with control group; °*P* < 0.05 and °°°*P* < 0.001 when WT vs. C1qa$^{-/-}$ mice treated with Dianeal-PD-4 are compared.

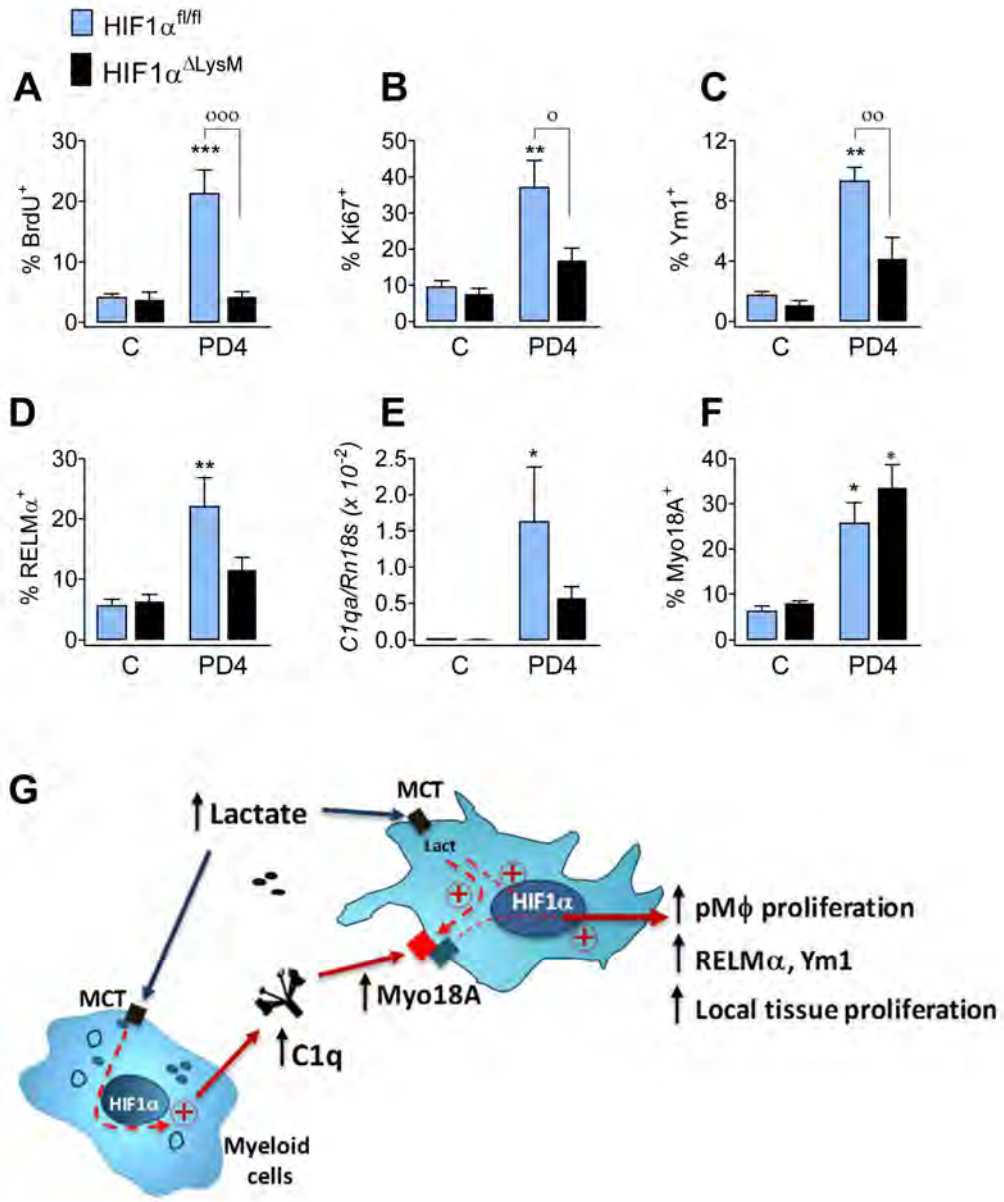

Fig. S9. Lactate-dependent proliferation and type 2 macrophage activation requires stabilization of HIF1α in a model of peritoneal dialysis. *Hif1a*$^{flox/flox}$*;LysMcre*$^{+/-}$ mice and littermate WT controls (*Hif1a*$^{flox/flox}$*;LysMcre*$^{-/-}$) were either untreated (control, C) or treated with 5 ip injections of Dianeal PD-4 every other day. Samples were analyzed a day after the last delivery. (**A**) BrdU incorporation in pMϕ. (**B**) Ki67expression. (**C**) Ym1 and (**D**) RELMα expression. (**E**) Amplification of C1qa-encoding mRNA in peritoneal tissue. (**F**) Myo18A expression on the surface of peritoneal macrophages. Results are representative from two independent experiments (means ± SEM) (untreated: 3 mice, PD4: 4 mice). ANOVA followed by the Bonferroni multiple-comparison test or Student's t-test (A) was used. **P* < 0.05, ***P* < 0.01, and ****P* < 0.001 when compared with control group; °*P* < 0.05, °°*P* < 0.01, and °°°*P* < 0.001 when WT vs. myeloid specific HIF-1α-deficient mice treated with Dianeal PD-4 are compared. (**G**) **Schematic of lactate-dependent promotion of a type 2 macrophage phenotype, which is dependent on HIF1α and C1q in the peritoneal cavity**. A lactate-based dialysate increases C1q levels in the peritoneal cavity and expression of myosin 18A on the surface of pMϕ. Dialysate-induced proliferation of pMϕ and production of type 2 macrophage markers were blocked in C1q deficiency mice and animals lacking HIF1α in macrophages, but not in IL-4Rα deficient mice. The data suggests that C1q is required to amplify HIF1α-dependent lactate signaling, which promotes peritoneal fibrosis. (MCT: monocarboxylate transporter for lactate; HIF1α: hypoxia-inducible factor 1α)

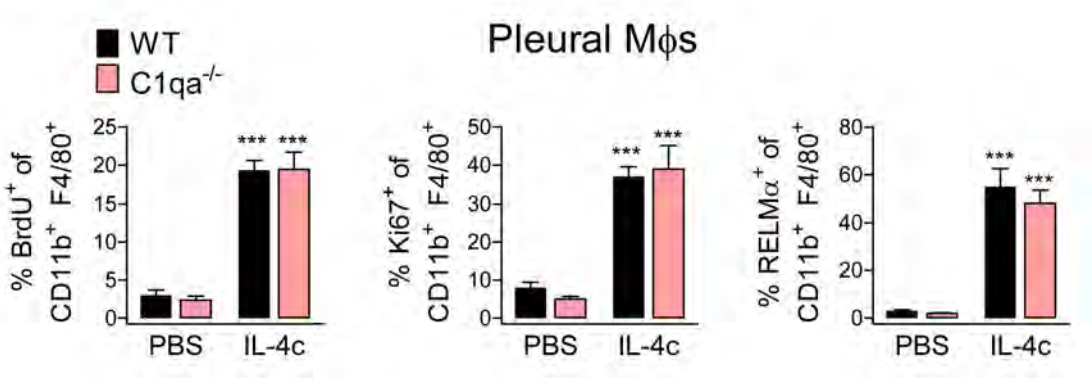

Fig. S10. IL-4 mediated proliferation and activation of pleural cavity macrophages is not enhanced by C1q. WT and C1qa-deficient mice were treated with 1μg of IL-4c (ip) at day 0; and samples were analyzed at day 1. Proliferation (BrdU incorporation and Ki67 expression) and M(IL-4) activation (RELMα expression) of resident pMϕ are shown. Data were pooled from two independent experiments (means ± SEM) (PBS: 8 mice, IL-4c: 10 mice). ANOVA followed by the Bonferroni multiple-comparison test was used. ***$P < 0.001$ when compared with the untreated group.

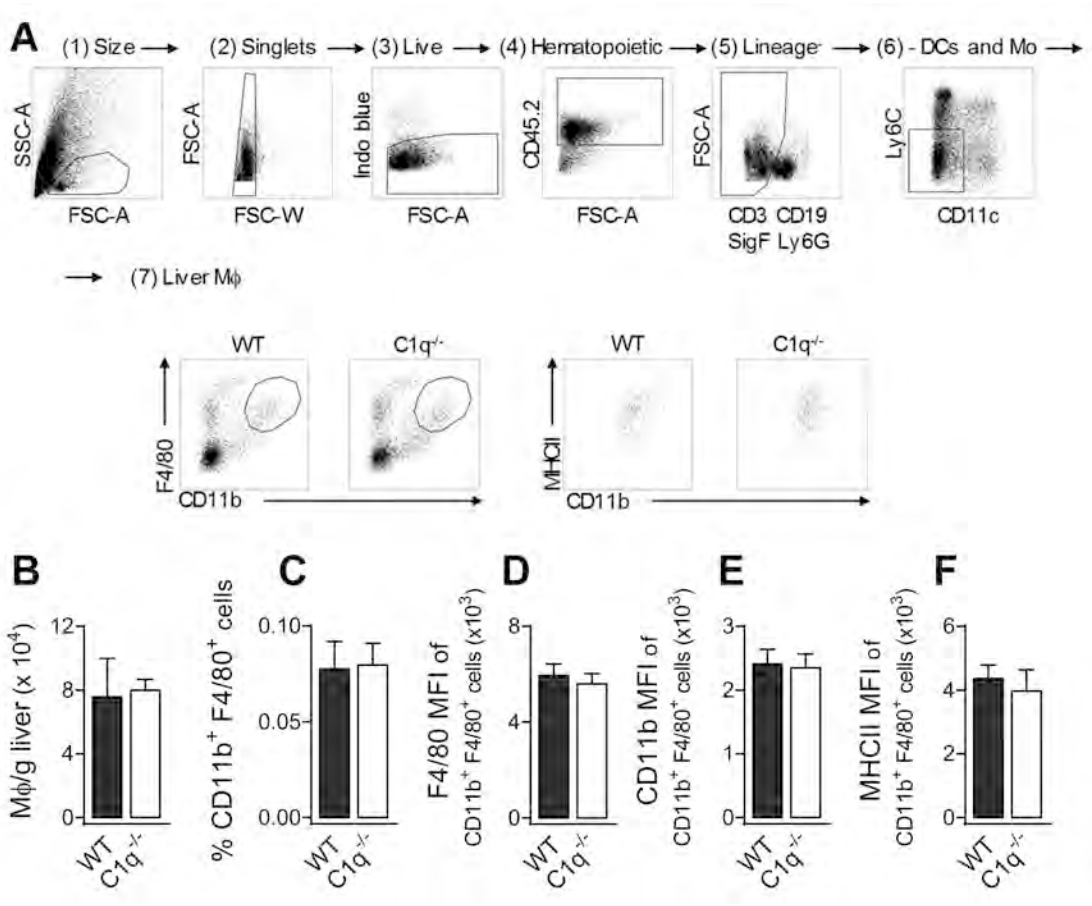

Fig. S11. Characterization of liver macrophages from C1q-deficient mice. (A) Sequential identification of liver macrophages by flow cytometry. Cells were first identified by size (1), and then as singlets (2) and live cells (3). Subsequently, hematopoietic cells were selected by CD45.2 expression (4). Lin^- cells (5) were obtained by gating out $CD3^+$, $CD19^+$, $Ly6G^+$ and $SiglecF^+$ cells (T cells, B cells, neutrophils and eosinophils, respectively). Monocytes and dendritic cells were successively excluded by expression of Ly6C and CD11c (6). Lin^-, $CD11c^-$ and $Ly6C^-$ populations were further subgated on the basis of the expression of CD11b versus F4/80. $CD11b^+$ and $F4/80^+$ cells are liver macrophages (7); a representative population of liver macrophages from WT and C1q-deficient mice is shown. The expression of MHCII and CD11b by liver macrophages is also shown for both mice strains. All shown gates are children of the parent gates shown previously. **(B)** Number and **(C)** percentage of liver macrophages from tissue homogenates. Expression of **(D)** F4/80, **(E)** CD11b, **(F)** MHCII, and **(G)** IL-4Rα in liver macrophages from WT and C1q-deficient mice. Data are representative of two independent experiments (mean ± SEM; WT: 4 mice, $C1qa^{-/-}$: 4 mice). Student's *t*-test was used.

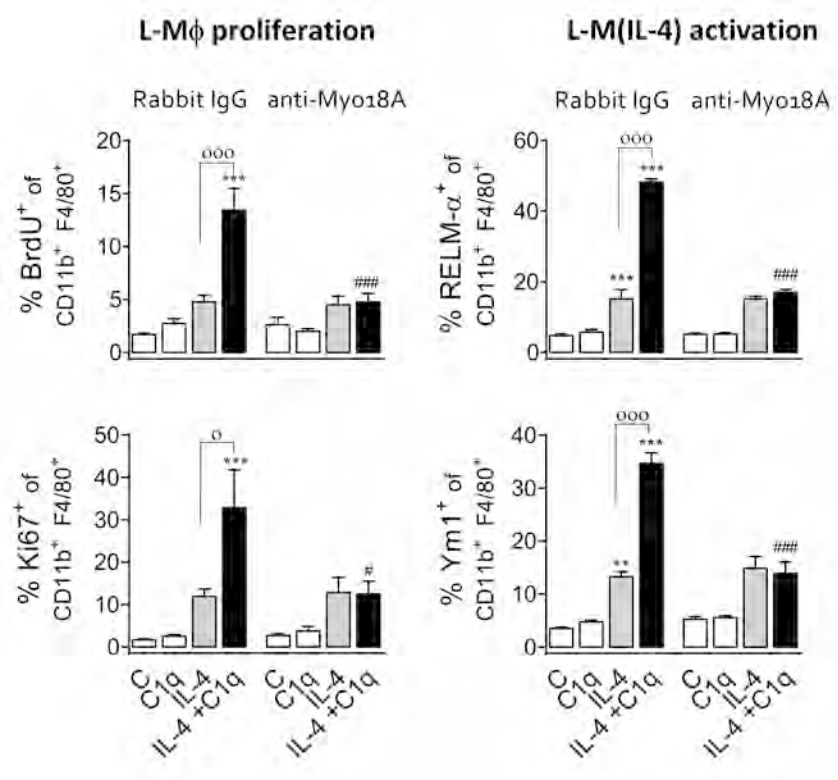

Fig. S12. Myo18A mediates C1q enhancement of IL-4-induced effects on liver macrophages. Purified mouse liver macrophages were treated with anti-Myo18A or rabbit IgG for one hour. Next, cells were IL-4-stimulated with or without C1q. Proliferation (BrdU incorporation and Ki67 expression) and M(IL-4) activation (RELMα and Ym1 expression) of liver macrophages are shown. The results are presented as means (± SEM) from three different cell cultures with at least three biological replicates. ANOVA followed by the Bonferroni multiple-comparison test was used. ***P* < 0.01, and ****P* < 0.001, when compared with untreated cells; °*P* < 0.05 and °°°*P* < 0.001, when C1q+IL4-treated macrophages were compared with IL-4-treated macrophages; #*P* < 0.05, and ###*P* < 0.001, when the effect of anti-Myo18A antibody is compared in cells treated with C1q+IL4.

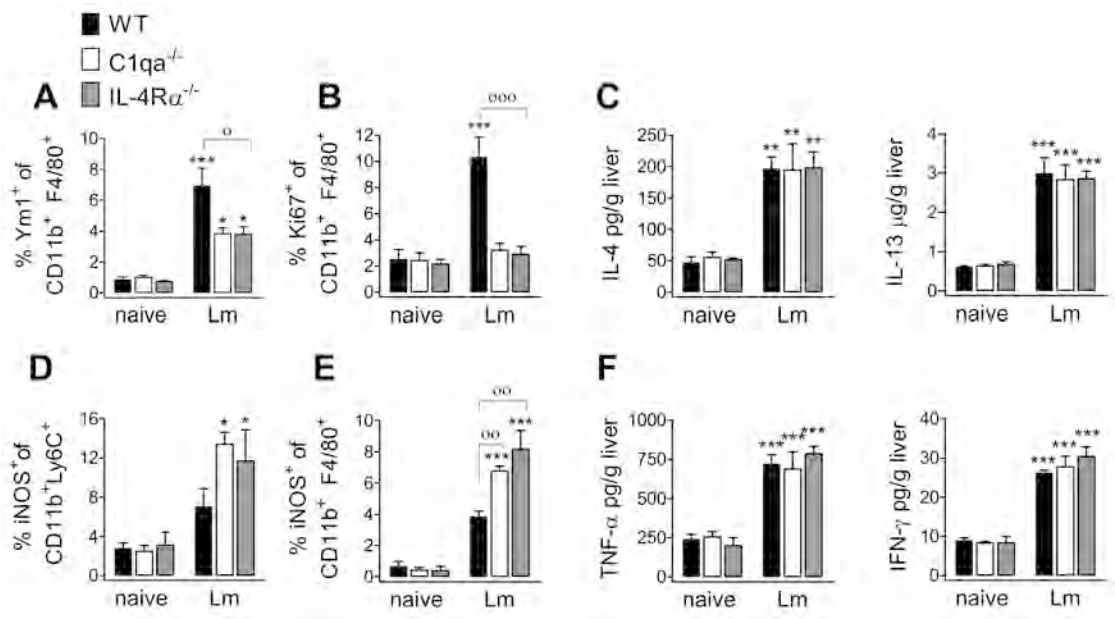

Fig. S13. Further characterization of WT vs. C1qa-deficient mice during *Listeria monocytogenes* infection. WT, C1qa$^{-/-}$, or IL-4Rα$^{-/-}$ mice were left uninfected or received intravenous infection with 10^4 *L. monocytogenes* c.f.u. and samples were assessed at day 3.5 after infection. **(A)** Expression of Ym1 by liver macrophages. **(B)** Ki67 expression by liver macrophages. **(C)** Levels of IL-4 and IL-13 in the supernatants of liver homogenates from WT, C1qa$^{-/-}$, and IL-4Rα$^{-/-}$ mice. **(D-E)** iNOS expression by liver monocytes and macrophages. **(C)** Levels of TNFα and IFN-γ in the supernatants of liver homogenates from WT, C1qa$^{-/-}$, and IL-4Rα$^{-/-}$ mice. Data are representative from two independent experiments (mean ± SEM; naïve: 4 mice, *Lm*: 4-6 mice). ANOVA followed by the Bonferroni multiple-comparison test was used. *p < 0.05, **p < 0.01 and ***p < 0.001, when compared with the uninfected group; °p < 0.05, °°p < 0.01, and °°°p < 0.001 when WT vs. C1qa$^{-/-}$ or IL-4Rα$^{-/-}$ infected groups are compared.

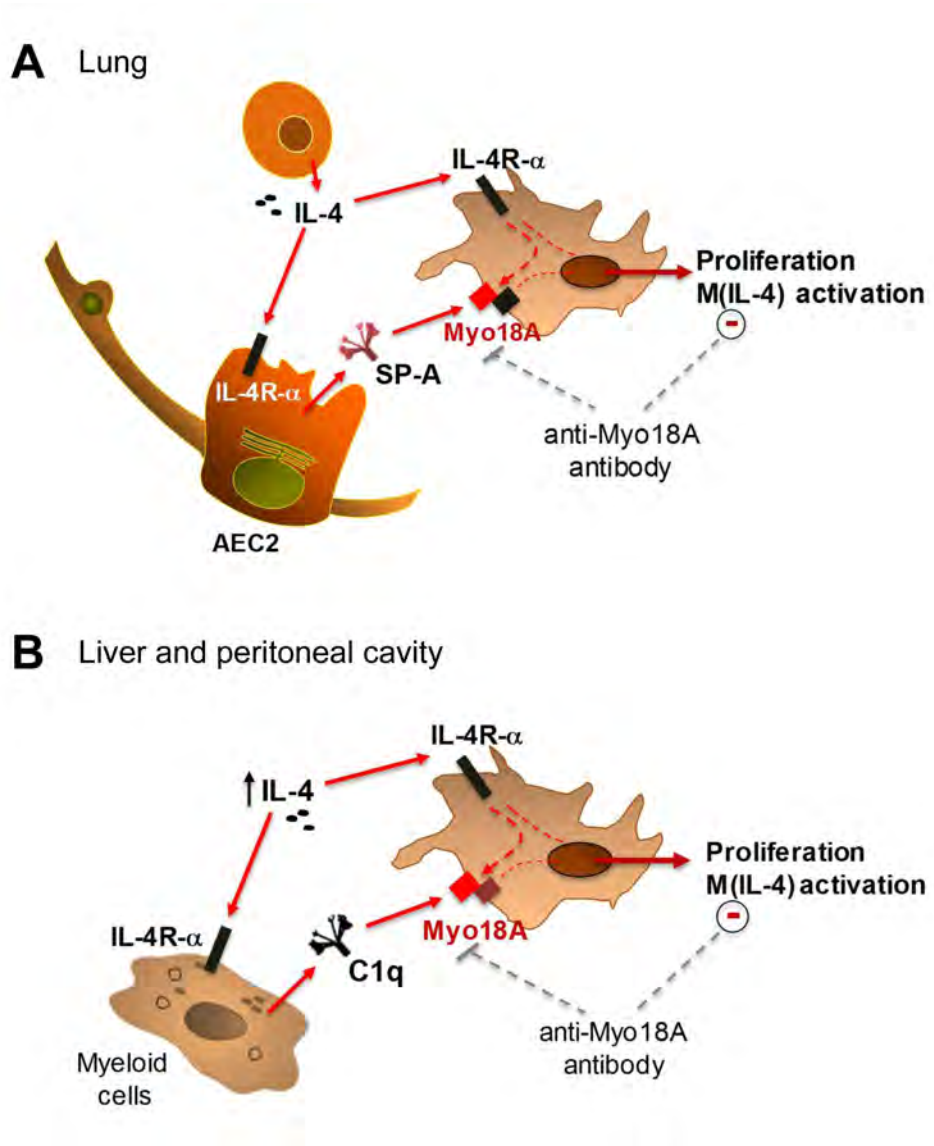

Fig. S14. Schematic of direct and indirect effects of IL-4. Rather than IL-4 (or IL-13) signaling to macrophages alone, IL-4 drives the production of a second signal for full M(IL-4) activation and proliferation. (**A**) IL-4 increases the production of SP-A by alveolar epithelial type II cells (AEC2) and the expression of myosin 18A on the surface of aMϕ. SP-A deficiency or receptor blockade abrogated IL-4-induced proliferation of aMϕ and reduced M(IL-4) activation. **(B)** In the liver and the peritoneal cavity, IL-4 increases the production of C1q and the expression of myosin 18A receptor on the surface of liver and peritoneal macrophages. C1q deficiency or receptor blockade impedes full M(IL-4) activation and proliferation.

Supplementary Table 1. Genotyping of the *Sftpa1*$^{-/-}$ and *Sftpa1*$^{+/+}$ littermates

SP-A-deficient mice genotyping	
Primer	Sequence
Sftpa1 F neo	GTGGGGTGGGATTAGATAAATGC
Sftpa1 1743-1766	GCATTAGACGACAGAACTCCAGCC
Sftpa1 R 1981-1957	TACTGAGAGATGTGTGCTTGGTGAG

Supplementary Table 2. Primer sequences used for quantitative RT-PCR of genes of interest.

Gene	Primer	Sequence
Sftpa1	For	CTGGAGAACATGGAGACAAGG
	Rev	AAGCTCCTCATCCAGGTAAGC
Col3a1	For	AAGGGTGAAGTCGGTGCTC
	Rev	TCCAGCTCCACCTCTAGCA
Col1a1	For	TCTGGTCTCCAGGGTCCTC
	Rev	GTCTTTGCCAGGAGAACCAG
Acta2	For	CCAACCGGGAGAAAATGAC
	Rev	CAGTTGTACGTCCAGAGGCATA
Vegf	For	ACTCGGATGCCGACACGGGA
	Rev	CCTGGCCTTGCTTGCTCCCC
Mmp12	For	CAATTGGAATATGACCCCCTGT
	Rev	AGCAAGCACCCTTCACTACAT
Rpl13a	For	CATGAGGTCGGGTGGAAGTA
	Rev	GCCTGTTTCCGTAACCTCAA
Rn18s	For	GTAACCCGTTGAACCCCATT
	Rev	CCATCCAATCGGTAGTAGCG
MKI67	For	TCGACCCTACAGAGTGCTCA
	Rev	GTGGGGAGCAGAGGTTCTTC
MRC1	For	CAGATGCCCGGAGTCAGATC
	Rev	TTTATCCACAGCCACGTCCC
GAPDH	For	GATCATGAGCAATGCCTCCT
	Rev	TGTGGTCATGAGTCGTTCCA

References

1. P. J. Murray, J. E. Allen, S. K. Biswas, E. A. Fisher, D. W. Gilroy, S. Goerdt, S. Gordon, J. A. Hamilton, L. B. Ivashkiv, T. Lawrence, M. Locati, A. Mantovani, F. O. Martinez, J.-L. Mege, D. M. Mosser, G. Natoli, J. P. Saeij, J. L. Schultze, K. A. Shirey, A. Sica, J. Suttles, I. Udalova, J. A. van Ginderachter, S. N. Vogel, T. A. Wynn, Macrophage activation and polarization: Nomenclature and experimental guidelines. *Immunity* **41**, 14–20 (2014). doi:10.1016/j.immuni.2014.06.008 Medline

2. R. K. Grencis, Immunity to helminths: Resistance, regulation, and susceptibility to gastrointestinal nematodes. *Annu. Rev. Immunol.* **33**, 201–225 (2015). doi:10.1146/annurev-immunol-032713-120218 Medline

3. F. Chen, Z. Liu, W. Wu, C. Rozo, S. Bowdridge, A. Millman, N. Van Rooijen, J. F. Urban Jr., T. A. Wynn, W. C. Gause, An essential role for TH2-type responses in limiting acute tissue damage during experimental helminth infection. *Nat. Med.* **18**, 260–266 (2012). doi:10.1038/nm.2628 Medline

4. T. A. Wynn, K. M. Vannella, Macrophages in Tissue Repair, Regeneration, and Fibrosis. *Immunity* **44**, 450–462 (2016). doi:10.1016/j.immuni.2016.02.015 Medline

5. J. R. Wright, Immunoregulatory functions of surfactant proteins. *Nat. Rev. Immunol.* **5**, 58–68 (2005). doi:10.1038/nri1528 Medline

6. A. J. Tenner, Membrane receptors for soluble defense collagens. *Curr. Opin. Immunol.* **11**, 34–41 (1999). doi:10.1016/S0952-7915(99)80007-7 Medline

7. D. Rückerl, J. E. Allen, Macrophage proliferation, provenance, and plasticity in macroparasite infection. *Immunol. Rev.* **262**, 113–133 (2014). doi:10.1111/imr.12221 Medline

8. H. Goto, J. G. Ledford, S. Mukherjee, P. W. Noble, K. L. Williams, J. R. Wright, The role of surfactant protein A in bleomycin-induced acute lung injury. *Am. J. Respir. Crit. Care Med.* **181**, 1336–1344 (2010). doi:10.1164/rccm.200907-1002OC Medline

9. E. N. Atochina, J. M. Beck, A. M. Preston, A. Haczku, Y. Tomer, S. T. Scanlon, T. Fusaro, J. Casey, S. Hawgood, A. J. Gow, M. F. Beers, Enhanced lung injury and delayed clearance of Pneumocystis carinii in surfactant protein A-deficient mice: Attenuation of cytokine responses and reactive oxygen-nitrogen species. *Infect. Immun.* **72**, 6002–6011 (2004). doi:10.1128/IAI.72.10.6002-6011.2004 Medline

10. J. G. Ledford, A. M. Pastva, J. R. Wright, Review: Collectins link innate and adaptive immunity in allergic airway disease. *Innate Immun.* **16**, 183–190 (2010). doi:10.1177/1753425910368446 Medline

11. C. M. Minutti, B. García-Fojeda, A. Sáenz, M. de Las Casas-Engel, R. Guillamat-Prats, A. de Lorenzo, A. Serrano-Mollar, Á. L. Corbí, C. Casals, Surfactant Protein A Prevents IFN-γ/IFN-γ Receptor Interaction and Attenuates Classical Activation of Human Alveolar Macrophages. *J. Immunol.* **197**, 590–598 (2016). doi:10.4049/jimmunol.1501032 Medline

12. M. Ikegami, J. A. Whitsett, A. Jobe, G. Ross, J. Fisher, T. Korfhagen, Surfactant metabolism in SP-D gene-targeted mice. *Am. J. Physiol. Lung Cell. Mol. Physiol.* **279**, L468–L476 (2000). Medline

13. S. Thawer, J. Auret, C. Schnoeller, A. Chetty, K. Smith, M. Darby, L. Roberts, R.-M. Mackay, H. J. Whitwell, J. F. Timms, J. Madsen, M. E. Selkirk, F. Brombacher, H. W. Clark, W. G. C. Horsnell, Surfactant Protein-D Is Essential for Immunity to Helminth Infection. *PLOS Pathog.* **12**, e1005461 (2016). doi:10.1371/journal.ppat.1005461 Medline

14. S. Guzik-Lendrum, S. M. Heissler, N. Billington, Y. Takagi, Y. Yang, P. J. Knight, E. Homsher, J. R. Sellers, Mammalian myosin-18A, a highly divergent myosin. *J. Biol. Chem.* **288**, 9532–9548 (2013). doi:10.1074/jbc.M112.441238 Medline

15. A. De Masson, J. Giustiniani, A. Marie-Cardine, J. D. Bouaziz, N. Dulphy, D. Gossot, P. Validire, A. Tazi, C. Garbar, M. Bagot, Y. Merrouche, A. Bensussan, Identification of CD245 as myosin 18A, a receptor for surfactant A: A novel pathway for activating human NK lymphocytes. *OncoImmunology* **5**, e1127493 (2016). doi:10.1080/2162402X.2015.1127493 Medline

16. C. H. Yang, J. Szeliga, J. Jordan, S. Faske, Z. Sever-Chroneos, B. Dorsett, R. E. Christian, R. E. Settlage, J. Shabanowitz, D. F. Hunt, J. A. Whitsett, Z. C. Chroneos, Identification of the surfactant protein A receptor 210 as the unconventional myosin 18A. *J. Biol. Chem.* **280**, 34447–34457 (2005). doi:10.1074/jbc.M505229200 Medline

17. F. Petry, M. Botto, R. Holtappels, M. J. Walport, M. Loos, Reconstitution of the complement function in C1q-deficient (C1qa-/-) mice with wild-type bone marrow cells. *J. Immunol.* **167**, 4033–4037 (2001). doi:10.4049/jimmunol.167.7.4033 Medline

18. J. Wang, Z.-P. Jiang, N. Su, J.-J. Fan, Y.-P. Ruan, W.-X. Peng, Y.-F. Li, X.-Q. Yu, The role of peritoneal alternatively activated macrophages in the process of peritoneal fibrosis related to peritoneal dialysis. *Int. J. Mol. Sci.* **14**, 10369–10382 (2013). doi:10.3390/ijms140510369 Medline

19. A. Pletinck, R. Vanholder, N. Veys, W. Van Biesen, Protecting the peritoneal membrane: Factors beyond peritoneal dialysis solutions. *Nat. Rev. Nephrol.* **8**, 542–550 (2012). doi:10.1038/nrneph.2012.144 Medline

20. T. Bellón, V. Martínez, B. Lucendo, G. del Peso, M. J. Castro, L. S. Aroeira, A. Rodríguez-Sanz, M. Ossorio, R. Sánchez-Villanueva, R. Selgas, M. A. Bajo, Alternative activation of macrophages in human peritoneum: Implications for peritoneal fibrosis. *Nephrol. Dial. Transplant.* **26**, 2995–3005 (2011). doi:10.1093/ndt/gfq771 Medline

21. J. M. Shipley, R. L. Wesselschmidt, D. K. Kobayashi, T. J. Ley, S. D. Shapiro, Metalloelastase is required for macrophage-mediated proteolysis and matrix invasion in mice. *Proc. Natl. Acad. Sci. U.S.A.* **93**, 3942–3946 (1996). doi:10.1073/pnas.93.9.3942 Medline

22. J. Lu, X. Wu, B. K. Teh, The regulatory roles of C1q. *Immunobiology* **212**, 245–252 (2007). doi:10.1016/j.imbio.2006.11.008 Medline

23. O. R. Colegio, N.-Q. Chu, A. L. Szabo, T. Chu, A. M. Rhebergen, V. Jairam, N. Cyrus, C. E. Brokowski, S. C. Eisenbarth, G. M. Phillips, G. W. Cline, A. J. Phillips, R. Medzhitov, Functional polarization of tumour-associated macrophages by tumour-derived lactic acid. *Nature* **513**, 559–563 (2014). doi:10.1038/nature13490 Medline

24. S. Watanabe, K. Sato, N. Hasegawa, T. Kurihara, K. Matsutani, K. Sanada, T. Hamaoka, S. Fujita, M. Iemitsu, Serum C1q as a novel biomarker of sarcopenia in older adults. *FASEB J.* **29**, 1003–1010 (2015). doi:10.1096/fj.14-262154 Medline

25. C. Shi, P. Velázquez, T. M. Hohl, I. Leiner, M. L. Dustin, E. G. Pamer, Monocyte trafficking to hepatic sites of bacterial infection is chemokine independent and directed by focal intercellular adhesion molecule-1 expression. *J. Immunol.* **184**, 6266–6274 (2010). doi:10.4049/jimmunol.0904160 Medline

26. C. Blériot, T. Dupuis, G. Jouvion, G. Eberl, O. Disson, M. Lecuit, Liver-resident macrophage necroptosis orchestrates type 1 microbicidal inflammation and type-2-mediated tissue repair during bacterial infection. *Immunity* **42**, 145–158 (2015). doi:10.1016/j.immuni.2014.12.020 Medline

27. S. J. Van Dyken, R. M. Locksley, Interleukin-4- and interleukin-13-mediated alternatively activated macrophages: Roles in homeostasis and disease. *Annu. Rev. Immunol.* **31**, 317–343 (2013). doi:10.1146/annurev-immunol-032712-095906 Medline

28. A. J. Byrne, T. M. Maher, C. M. Lloyd, Pulmonary Macrophages: A New Therapeutic Pathway in Fibrosing Lung Disease? *Trends Mol. Med.* **22**, 303–316 (2016). doi:10.1016/j.molmed.2016.02.004 Medline

29. J. Xue, V. Sharma, M. H. Hsieh, A. Chawla, R. Murali, S. J. Pandol, A. Habtezion, Alternatively activated macrophages promote pancreatic fibrosis in chronic pancreatitis. *Nat. Commun.* **6**, 7158 (2015). doi:10.1038/ncomms8158 Medline

30. J. M. Coya, H. T. Akinbi, A. Sáenz, L. Yang, T. E. Weaver, C. Casals, Natural anti-infective pulmonary proteins: In vivo cooperative action of surfactant protein SP-A and the lung antimicrobial peptide SP-BN. *J. Immunol.* **195**, 1628–1636 (2015). doi:10.4049/jimmunol.1500778 Medline

31. I. García-Verdugo, F. Sánchez-Barbero, F. U. Bosch, W. Steinhilber, C. Casals, Effect of hydroxylation and N187-linked glycosylation on molecular and functional properties of recombinant human surfactant protein A. *Biochemistry* **42**, 9532–9542 (2003). doi:10.1021/bi0347196 Medline

32. F. Sánchez-Barbero, G. Rivas, W. Steinhilber, C. Casals, Structural and functional differences among human surfactant proteins SP-A1, SP-A2 and co-expressed SP-A1/SP-A2: Role of supratrimeric oligomerization. *Biochem. J.* **406**, 479–489 (2007). doi:10.1042/BJ20070275 Medline

33. F. Sánchez-Barbero, J. Strassner, R. García-Cañero, W. Steinhilber, C. Casals, Role of the degree of oligomerization in the structure and function of human surfactant protein A. *J. Biol. Chem.* **280**, 7659–7670 (2005). doi:10.1074/jbc.M410266200 Medline

34. G. Li, J. Siddiqui, M. Hendry, J. Akiyama, J. Edmondson, C. Brown, L. Allen, S. Levitt, F. Poulain, S. Hawgood, Surfactant protein-A—deficient mice display an exaggerated early inflammatory response to a beta-resistant strain of influenza A virus. *Am. J. Respir. Cell Mol. Biol.* **26**, 277–282 (2002). doi:10.1165/ajrcmb.26.3.4584 Medline

35. F. Carlucci, A. Ishaque, G. S. Ling, M. Szajna, A. Sandison, P. Donatien, H. T. Cook, M. Botto, C1q Modulates the Response to TLR7 Stimulation by Pristane-Primed

Macrophages: Implications for Pristane-Induced Lupus. *J. Immunol.* **196**, 1488–1494 (2016). doi:10.4049/jimmunol.1401009 Medline

36. D. R. Herbert, C. Hölscher, M. Mohrs, B. Arendse, A. Schwegmann, M. Radwanska, M. Leeto, R. Kirsch, P. Hall, H. Mossmann, B. Claussen, I. Förster, F. Brombacher, Alternative macrophage activation is essential for survival during schistosomiasis and downmodulates T helper 1 responses and immunopathology. *Immunity* **20**, 623–635 (2004). doi:10.1016/S1074-7613(04)00107-4 Medline

37. A. A. Thompson, P. M. Elks, H. M. Marriott, S. Eamsamarng, K. R. Higgins, A. Lewis, L. Williams, S. Parmar, G. Shaw, E. E. McGrath, F. Formenti, F. J. Van Eeden, V. L. Kinnula, C. W. Pugh, I. Sabroe, D. H. Dockrell, E. R. Chilvers, P. A. Robbins, M. J. Percy, M. C. Simon, R. S. Johnson, S. A. Renshaw, M. K. B. Whyte, S. R. Walmsley, Hypoxia-inducible factor 2α regulates key neutrophil functions in humans, mice, and zebrafish. *Blood* **123**, 366–376 (2014). doi:10.1182/blood-2013-05-500207 Medline

38. S. J. Jenkins, D. Ruckerl, P. C. Cook, L. H. Jones, F. D. Finkelman, N. van Rooijen, A. S. MacDonald, J. E. Allen, Local macrophage proliferation, rather than recruitment from the blood, is a signature of TH2 inflammation. *Science* **332**, 1284–1288 (2011). doi:10.1126/science.1204351 Medline

39. S. J. Jenkins, D. Ruckerl, G. D. Thomas, J. P. Hewitson, S. Duncan, F. Brombacher, R. M. Maizels, D. A. Hume, J. E. Allen, IL-4 directly signals tissue-resident macrophages to proliferate beyond homeostatic levels controlled by CSF-1. *J. Exp. Med.* **210**, 2477–2491 (2013). doi:10.1084/jem.20121999 Medline

40. L. H. Jackson-Jones, D. Rückerl, F. Svedberg, S. Duncan, R. M. Maizels, T. E. Sutherland, S. J. Jenkins, H. J. McSorley, C. Bénézech, A. S. MacDonald, J. E. Allen, IL-33 delivery induces serous cavity macrophage proliferation independent of interleukin-4 receptor alpha. *Eur. J. Immunol.* **46**, 2311–2321 (2016). doi:10.1002/eji.201646442 Medline

41. M. Camberis, G. Le Gros, J. Urban Jr., Animal model of Nippostrongylus brasiliensis and Heligmosomoides polygyrus. *Curr. Protoc. Immunol.* **Chapter 19**, 12 (2003). doi:10.1002/0471142735.im1912s55 Medline

42. M. J. Holland, Y. M. Harcus, P. L. Riches, R. M. Maizels, Proteins secreted by the parasitic nematode *Nippostrongylus brasiliensis* act as adjuvants for Th2 responses. *Eur. J. Immunol.* **30**, 1977–1987 (2000). doi:10.1002/1521-4141(200007)30:7<1977:AID-IMMU1977>3.0.CO;2-3 Medline

43. T. E. Sutherland, N. Logan, D. Rückerl, A. A. Humbles, S. M. Allan, V. Papayannopoulos, B. Stockinger, R. M. Maizels, J. E. Allen, Chitinase-like proteins promote IL-17-mediated neutrophilia in a tradeoff between nematode killing and host damage. *Nat. Immunol.* **15**, 1116–1125 (2014). doi:10.1038/ni.3023 Medline

44. C. Casals, J. Arias-Díaz, F. Valiño, A. Sáenz, C. García, J. L. Balibrea, E. Vara, Surfactant strengthens the inhibitory effect of C-reactive protein on human lung macrophage cytokine release. *Am. J. Physiol. Lung Cell. Mol. Physiol.* **284**, L466–L472 (2003). doi:10.1152/ajplung.00325.2002 Medline

45. W. Q. Zeng, J. Q. Zhang, Y. Li, K. Yang, Y. P. Chen, Z.-J. Liu, A new method to isolate and culture rat kupffer cells. *PLOS ONE* **8**, e70832 (2013). doi:10.1371/journal.pone.0070832 Medline

46. A. C. MacKinnon, S. L. Farnworth, P. S. Hodkinson, N. C. Henderson, K. M. Atkinson, H. Leffler, U. J. Nilsson, C. Haslett, S. J. Forbes, T. Sethi, Regulation of alternative macrophage activation by galectin-3. *J. Immunol.* **180**, 2650–2658 (2008). doi:10.4049/jimmunol.180.4.2650 Medline